



Covalent diphenylalanine peptide nanotube conjugated to folic acid/magnetic nanoparticles for anti-cancer drug delivery



Giti Emtiazi ^{a, b}, Tayebeh Zohrabi ^c, Lai Yeng Lee ^d, Neda Habibi ^{e, f, *}, Ali Zarrabi ^c

^a Department of Biotechnology, Faculty of Biological Science and Technology, Shahid Ashrafi Esfahani University, Iran

^b Department of Biology, Faculty of Science, University of Isfahan, Iran

^c Department of Biotechnology, Faculty of Advanced Sciences and Technologies, University of Isfahan, Isfahan, Iran

^d School of Chemical Engineering and Advanced Materials, Newcastle University, Singapore

^e Department of Biomedical Engineering, College of Engineering, The University of Texas at San Antonio, One UTSA Circle, San Antonio, TX 78249-0619, USA

^f Research Institute for Nanotechnology and Advanced Materials, Isfahan University of Technology, Iran

ARTICLE INFO

Article history:

Received 7 April 2017

Received in revised form

5 June 2017

Accepted 6 June 2017

Available online 7 June 2017

Keywords:

Diphenylalanine

Nanotubes

Peptide

Targeting

Drug delivery

ABSTRACT

Micro and nanotubes obtained from the self-assembly of diphenylalanine peptides (FNTs) were conjugated to folic acid/magnetic nanoparticles (FA/MNPs) and evaluated as a potential system for anti-cancer drug delivery. The conjugates were obtained by providing a covalent linkage through the amine groups on FNTs with the carboxylic groups on FA/MNPs. The anti-cancer therapeutic 5-fluorouracil (5-FU), and anti-inflammatory cargo flufenamic acid (FFA), were loaded in peptide arrays during their self-assembly in the liquid phase. AFM and CLSM analysis indicated the presence of FA aggregates on FNTs. The data revealed that the cargo 5-FU, was distributed in dendrite peptide nanotubes whereas the non-polar cargo FFA, was homogeneously embedded in the structure of large discrete micro tubes. FTIR spectra of FA-MNPs/FNTs showed peak of amide II at 1623 cm^{-1} indicating covalent interactions between amines and carboxylic groups and confirmed the successful conjugation of the nanoparticles and peptide assemblies. The results indicated that 5-FU has been released from FNTs within 4 h, and incorporation of 5-FU in FNTs hydrogels has significantly slowed the release rate within the first 2 h. Our approach offers a new pathway for cancer treatment in which several functionalities are embedded in a single carrier.

Published by Elsevier B.V.

1. Introduction

Di-phenylalanine (FF) is a dipeptide extracted from Alzheimer's polypeptide [1–6] as a core recognition motif for molecular self-assembly [3]. Formation of nanotubes from diphenylalanine (FNTs) were first reported by Reches and Gazit and since then FNTs has been used as a building block for formation of various functional nanostructures such as nanotubes, spherical vesicles and nanofibrils [7]. Typically, the self-assembly takes place by the aim of complex interaction of backbone–backbone hydrogen bonds and $\pi\cdots\pi$ interactions between the aromatic rings of the side-chains [8–10]. Nanotubes prepared from peptides are great alternatives over carbon nanotubes (CNT) for drug delivery purposes due to the associated risk of using CNT in human health [11,12].

The FF self-assembled structure could be designed with motifs

and ligands to become smart and stimuli-responsive, therefore achieving direct and triggered drug delivery to the site of disease [13–15]. Modified nanotubes are applicable in theranostic medicine which targeted delivery together with imaging organs and tissues offers the possibility of both diagnosis and treatments effectively [16]. The resulting nanosystems, are expected to play a significant role in future of translational medicine.

Among various targeting systems, folic acid (FA) provides a useful method for delivering therapeutic or imaging agents to tumors [17, 11, 18]. It is proven that most tumors overexpress the folate receptors (FR) at advanced stage, and therefore contain increased density of FR. The overexpression of FR occurs in many cancer types such as breast cancer, lung and brain. In addition to numerous drug delivery efforts, folate-targeted technology has been successfully applied to MRI contrast agents [18], fluorescence imaging of cancer cells [19, 17], and radio-imaging of therapeutic agents [20].

Furthermore, magnetic nanoparticles (MNPs) represent a major class of nanostructures with the potential to benefit current clinical diagnostic and therapeutic techniques. Due their unique properties,

* Corresponding author.

E-mail address: ned.habibi@gmail.com (N. Habibi).

MNPs are being actively investigated as the next generation of magnetic resonance imaging (MRI) contrast agents [21, 1] as carriers for targeted drug delivery and cancer treatments with hyperthermia [22]. Moreover, a less investigated aspect of MNPs is their potential for controlled release of cargos once exposed to an alternate magnetic field [23].

Several research groups have investigated conjugation of folic acid to nanoparticle and nanotubes. Covalent conjugations are mostly used for FA functionalization due to several advantages of covalent bindings toward non-covalent strategies such as stability at different physiological conditions [11, 24]. Castillo et al. studied the conjugation of folic acid to carbon nanotubes and demonstrated the uptake of CNT by THP-1 [24]. In another study, Zhang et al. used Gold nanoparticles (GNPs) modified with glutathione (GSH) in order to conjugate with folic acid through amino group of FA and carboxyl group of GSH [25]. Magnetic nanoparticles have been conjugated to folic acid as an effective method for the separation and detection of ovarian cancer cells. It is shown that the ability of FA to bind its receptor to allow endocytosis is not affected by covalent conjugation of small molecules [26]. Therefore, it is crucial to study the molecular structure of FF self-assembled nanostructures after binding with FA/MNPs. In this work, we combine the biocompatibility and biofunctionality of peptide nanotubes with targeting ligands of FA and MNPs and further evaluate its potential as a drug delivery vehicle.

Herein the carbodiimide/N-hydroxysuccinimide (EDC/NHS) chemistry has been utilized to covalently bond carboxyl groups of FA/MNPs to amine groups of FNTs. The conjugates were characterized using microscope and spectroscopy techniques. The results showed evidence of FA aggregates on peptide nanotube and peak of amide at 1630 cm^{-1} indicating a covalent conjugation. The morphology of self-assembled structures of diphenylalanine was effected by the polar and non-polar properties of the cargos which could greatly influence targeting FR receptors. We therefore argue that the synthesized peptide nanotube are suitable drug vehicles for loading 5-FU and have the potential to be used as co-delivery carriers.

2. Materials and methods

2.1. Materials

The lyophilized form of the L-diphenylalanine peptide (Code: P4126), Silicon wafers (Code: 204323), Gold coated silicon wafer (643262), Fluorouracil (5-FU), N-Hydroxysuccinimide Esters (NHS) (Code: 130672), were all obtained from Sigma–Aldrich. N-(3-Dimethylaminopropyl)-N'-ethylcarbodiimide hydrochloride (EDC) (code: 851007), 1,1,1,3,3,3-hexafluoro-2-propanol (HFIP) (Code: 804515) as solvent (99% purity), Iron (III) chloride hexahydrate ($\text{FeCl}_3 \cdot 6\text{H}_2\text{O}$), iron (II) sulfate heptahydrate ($\text{FeSO}_4 \cdot 7\text{H}_2\text{O}$), aqueous ammonia (28%) were purchased from Merck. Deionized water (18.2 $\text{M}\Omega \text{ cm}^{-1}$), was filtered by the Millipore Water system, and used throughout the experiment.

2.2. Synthesis of FNTs

A stock solution of FF was prepared in HFIP with concentration of 100 mg/ml. To synthesis FF self-assemble nanostructures, the stock solution was diluted to 2 mg/ml by adding deionized water and FNTs were immediately formed in solution. A drop was added to gold and silicone surfaces and left to dry. The FNTs synthesized in solution were analyzed by Zetasizer and FNTs on surfaces were imaged with AFM.

2.3. Synthesis of iron oxide MNPs modified with FA

Fe_3O_4 nanoparticles were prepared by chemical co-precipitation route. In a typical procedure, 5 g ferrous sulfate and 10 g ferric chloride and was dissolved into 25 ml of 2 M Hydrochloric acid in three-necked flask at 60 °C. Nitrogen was introduced during the synthesis to extrude the air and prevent oxidization of ferrous ions. 2 g folic acid in 2 ml water was added to reaction system to produce FA/MNPs. FA was added slowly for 30 min at 45 °C under nitrogen atmosphere and mild stirring condition [27]. Then 20 ml ammonium hydroxide (28%) was added drop wise into the iron solution under sonication and agitation for 40 min to ensure homogenous mixing. The pH was set to 9–11. After 1 h of stirring, the precipitant of Fe_3O_4 nanoparticles were collected by a permanent magnet, washed 2 times and dried in oven for 12 h.

2.4. Conjugation of FA/MNPs to FNTs with EDC

The conjugation was carried out through coupling carboxylic groups of FA to amines of FNTs with EDC. EDC is a common carbodiimide for activating carboxylic groups and binding biomolecules with carboxylic and amine groups [11]. To this aim, 20 mg FA/MNPs were put in contact with 2 mg/ml EDC in buffer pH = 5 for 1 h. The coupling reaction was carried out in the presence of sulfo-NHS to avoid formation of competing reaction by hydrolysis of the intermediate EDC-FA. 1 ml FNTs were put in contact with 0.2 ml of activated FA/MNPs for 4 h and subsequently centrifuged at 3000 rpm for 20 min and washed by distilled water.

2.5. Fluorouracil (5-FU) loadings of FNTs

The potential of FNTs as anti-cancer drug-delivery carriers were evaluated with fluorouracil. Loading 5-FU were carried out during the process of FNT self-assembly. 5-FU at concentration of 25 $\mu\text{g}/\text{ml}$ was added to the mixture of FNT, leading to the spontaneous accommodation of the cargo within the tubes. The solvent was left to dry overnight at room temperature, and the assemblies were then cleaned with ultrapure water several times to eliminate residual 5-FU. The anti-inflammatory non-polar cargo flufenamic acid (FFA), were loaded within FNTs with the same approach at concentrations of 25 $\mu\text{g}/\text{ml}$.

2.6. Fluorouracil (5-FU) release from FNT hydrogels

In vitro release assays were performed using FNT hydrogels prepared in a mixture of 75% toluene and 25% ethanol. A stock solution of FNTs (100 mg/ml) were mixed with solvent (75% toluene and 25% ethanol) in a ratio of 2:100 and were left to form hydrogels for 4 h fluorouracil in concentration of 25 $\mu\text{g}/\text{ml}$ were further added to hydrogel mixture and were kept for 3 h to allow efficient loading. Samples of FNT hydrogels loaded with 5-FU, were centrifuged at 6000 rpm for 20 min and loading efficiency was analyzed by UV spectrophotometer. FNT hydrogels were carefully put in contact with PBS and left for 3 h. At each intervals samples of PBS were taken and % release of 5-FU was measured with UV-VIS spectrophotometer.

2.7. Cell viability studies

MCF-7 were cultivated on 75 cm^2 flasks in DMEM supplemented with 10% FBS, 100 IU/ml penicillin, and 100 $\mu\text{g}/\text{mL}$ streptomycin. Flasks were incubated at 37° C and in an atmosphere of 5% CO_2 . After 24 h the medium was first aspirated out, and then cells were rinsed with 3 mL of PBS and trypsinized with trypsin-EDTA to

disassociate the cells from the flask. Medium (3 mL) containing 10% of serum was added to the flask to stop the reaction of trypsin. Cells were incubated in 5% CO₂ at 37° C for 24 h. FA/MNPs/FNTs prepared in water at a starting concentration of 1000 µg/mL and were sterilized and dried in an oven at 80 °C, then rehydrated with DMEM (1 mL) at room temperature. Samples of FA/MNPs and FNTs/5-FU were prepared and sterilized. 100 µL of each sample were added to cells in a 96-well microplate and were incubated for 24 h. Then cell culture medium was removed and fresh medium and 10 µL of MTT (5 mg/mL in PBS) were added into each well. Cells were incubated at 37° C and then solution was removed after a 4-h exposure, and rinsed with 100 µL of PBS. 100 µL of DMSO was added to each well, and plates were incubated 1 h until all formazan crystals had been dissolved. The absorbance of each well was determined in Awareness Technology Stat Fax 2100 Microplate Reader (STAT-FAX-2100) at 490 nm.

2.8. Characterization

Atomic Force Microscopy (AFM) was used to characterize FA/MNPs nanoparticles and FNTs modified with FA/MNPs. AFM imaging was performed with a dual scope C-26, DME Germany equipped with C-26 controller in tapping mode (Danish Micro Engineering, Denmark). Standard silicon Multi75Al tips with resonance frequencies and spring constants of about 75 kHz and 2.84 N m⁻¹ respectively were used for imaging under ambient conditions. Field emission scanning electron microscope micrographs were taken using a FE-SEM, Hitachi model S-4160 [28, 29].

Fourier Transform Infrared (FTIR) spectra of FNTs/5-FU modified with FA/MNPs were recorded using KBr disks on a FTIR 6300 [30, 31].

Fluorescence measurements were carried by Fluorescence Microscope Leica (Leica DFC3000 G) equipped with dedicated fluorescence CCD sensor and Digital monochrome camera. The emission spectra were obtained by exciting the samples at 390 nm and scanning the emission from 402 to 480 nm. The fluorescence images of FNTs/5-FU nanotubes and FA/MNPs were also obtained by using confocal laser scanning microscope with a total of 4 microscopes: 1 Olympus FV300, 2 Olympus FV1000, 1 Lsm510 Meta at $\lambda_{ex} = 490$ nm and emission collected at a range of 480–590 nm. The equipment is able to obtain images with clarity and reasonable resolution; thus enabling 3-D reconstruction of the specimen from a series of optical section images obtained. The images were analyzed with Olympus Fluoview 4 viewer software. Size distribution of the assembled nanostructures in solution was analyzed by DLS using Malvern Zetasizer Nano ZS. The experiment was carried out using a 633 nm laser at 25 °C.

3. Results and discussion

AFM images of MNPs functionalized with FA are shown in Fig. 1. The morphology and mean size of synthesized MNPs were presented in these images indicating the particles were spherical, non-aggregated with a mean size of 100 nm. To further characterize FA/MNPs, confocal fluorescence microscopy was used. Folic acid is a biomolecule that shows strong emission fluorescence at

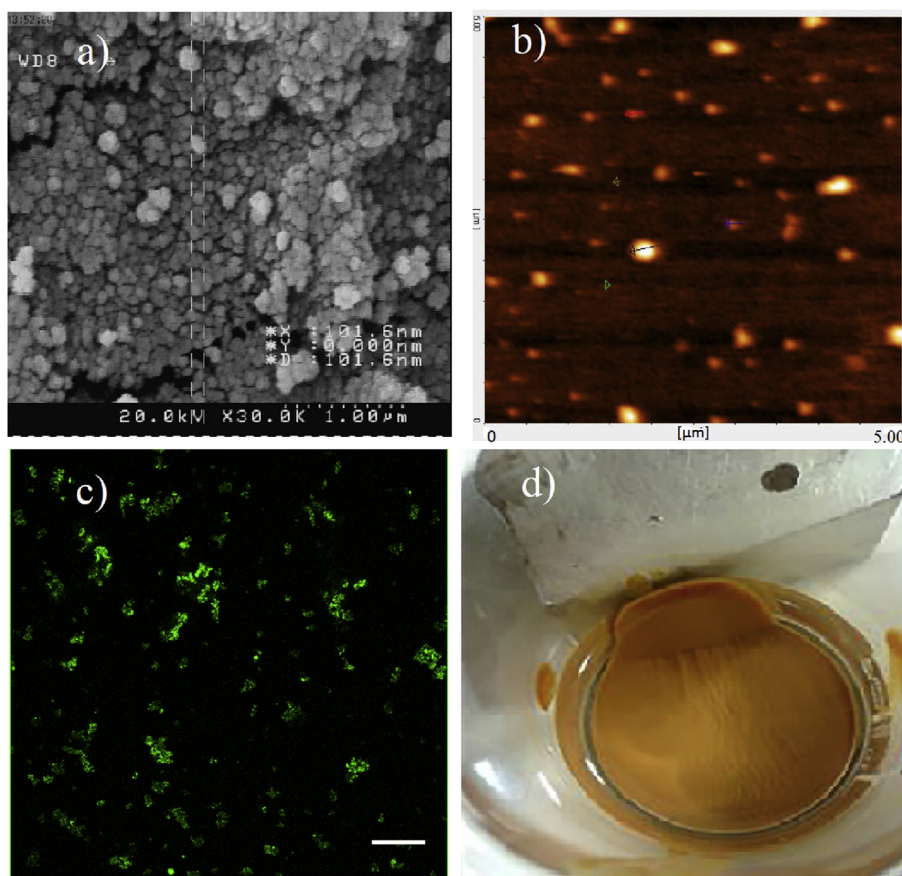


Fig. 1. From left to right: a) FE-SEM image of MNPs. b) AFM image of MNPs functionalization with FA; c) Confocal fluorescence image of FA/MNPs (Scale bar 2 µm); d) FA/MNPs collected by magnetic field.

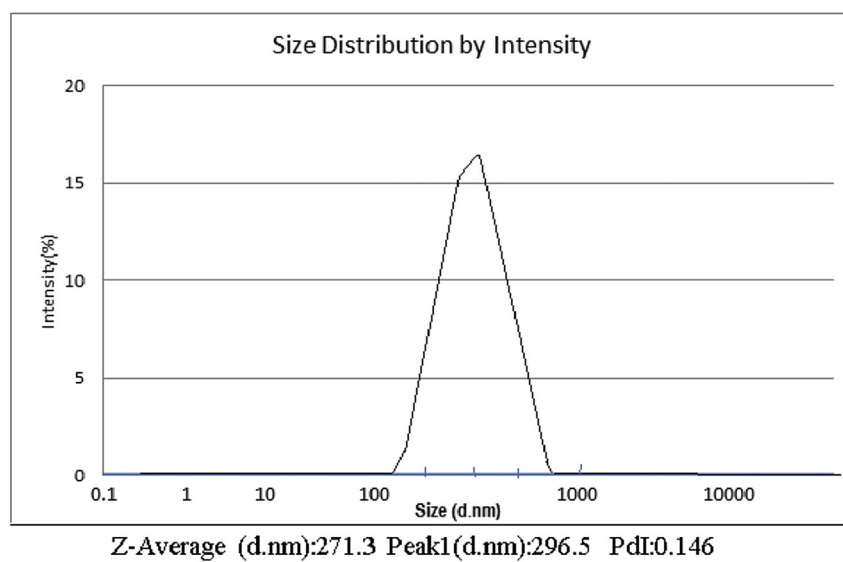
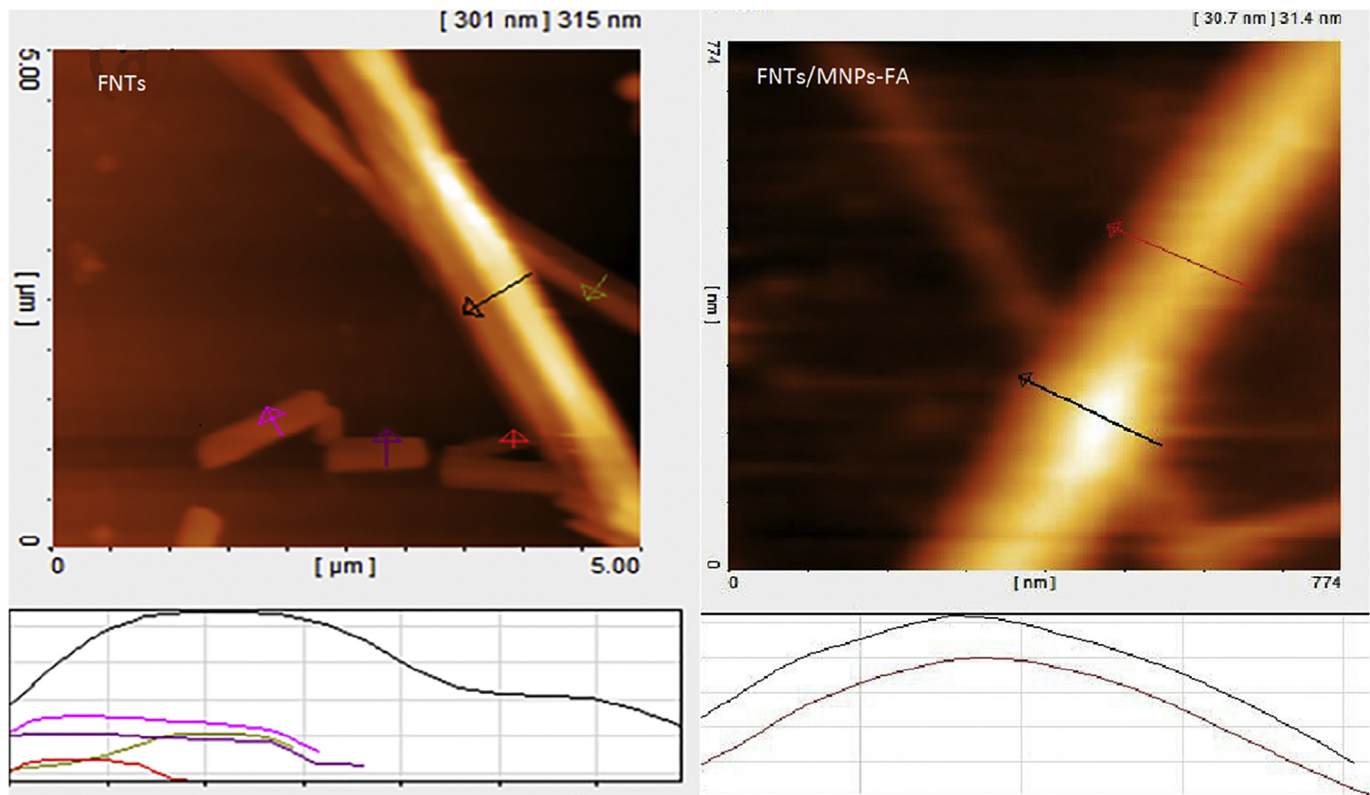


Fig. 2. a) AFM image of FNTs formed on Si substrates. FNTs modified with FA/MNPs showing MNPs embedded inside FNTs. Size distribution of diphenylalanine (FF) self-assembled structures in HFIP after 24 h (hydrodynamic diameter 296 nm).

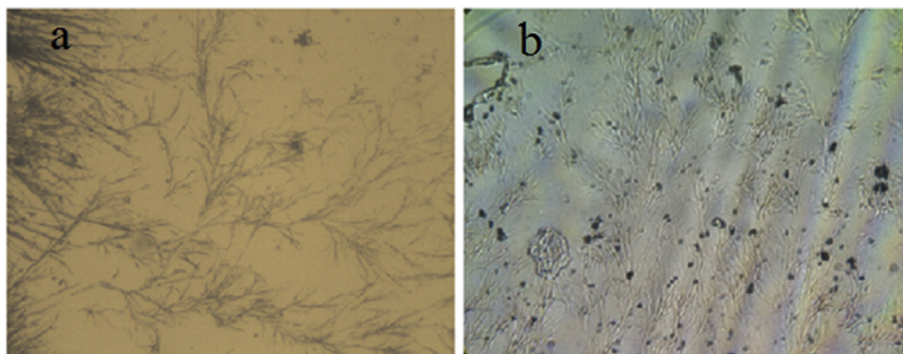


Fig. 3. a) Optical microscope image of FF dendrites spread on glass. b) Optical image of MNPs attached to the wall of FNTs.

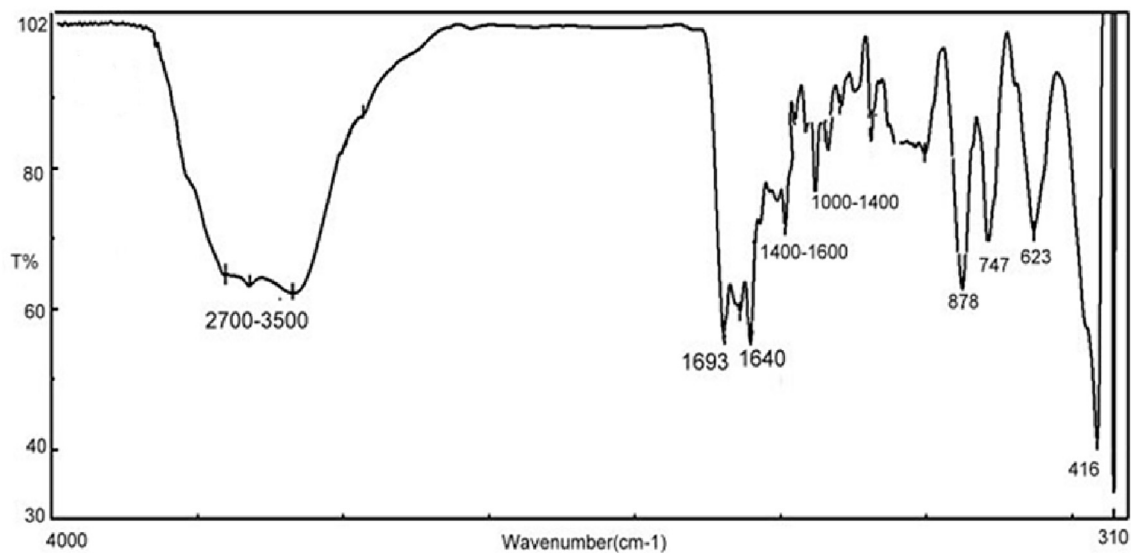


Fig. 4. FTIR spectra of FNTs modified with FA/MNPs.

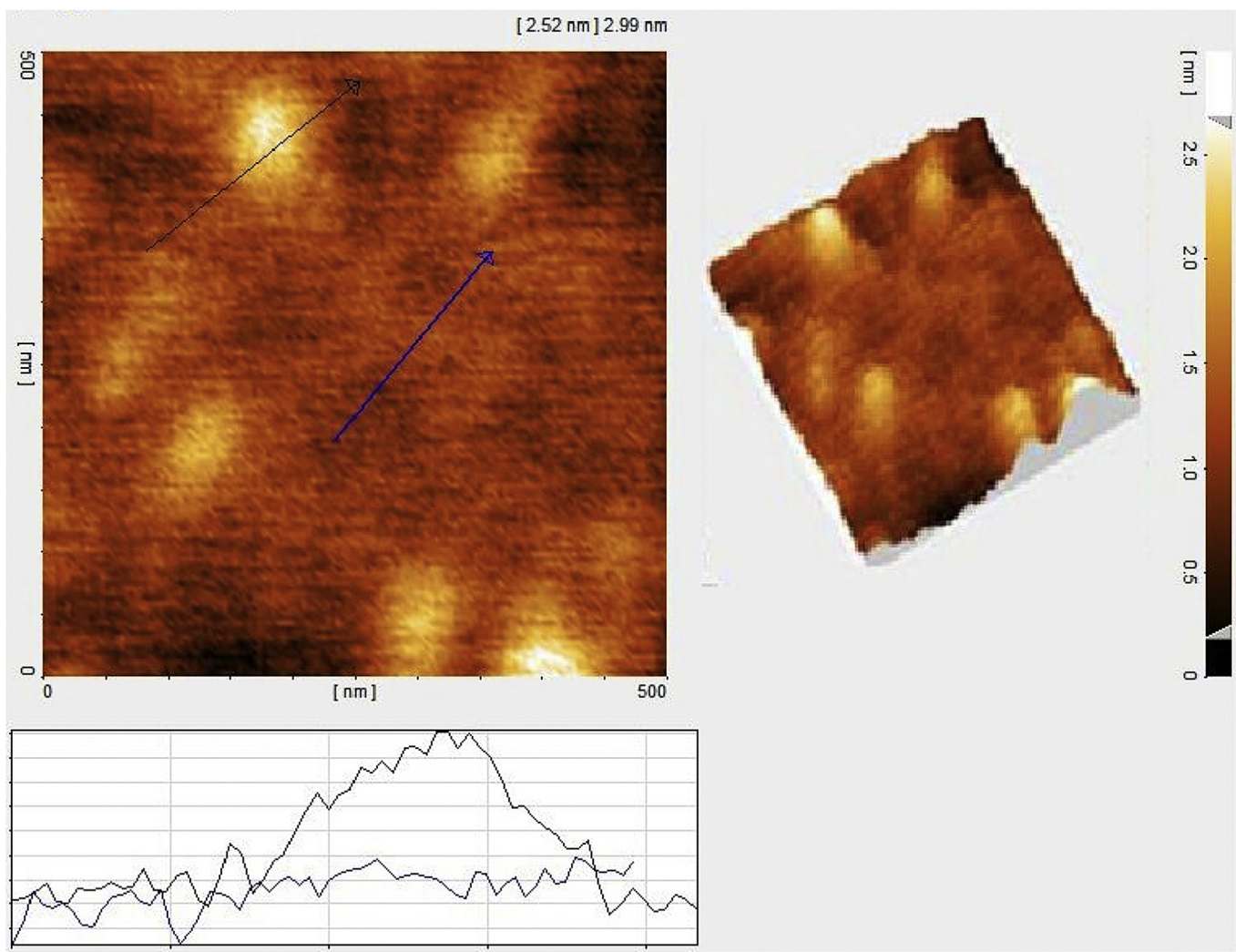


Fig. 5. FNTs modified with FA/MNPs transition into vesicle nanostructures by diluting FNTs solution.

$\lambda = 480$ nm [11]. The uniform and strong fluorescence emission intensity of FA on MNPs indicated homogeneous distribution of FA on MNPs (Fig. 1). Similar effects have been previously reported using Gold nanoparticles (GNPs) conjugated with folic acid. The observed fluorescence from FA/MNPs conjugates is an evidence of successful decoration of MNPs with FA. MNPs modified with folic acid were collected using a magnetic field indicating the coating has not affected magnetic properties of Fe_3O_4 NPs (Fig. 1c).

AFM images of FNTs before and after conjugation with FA/MNPs are displayed in Fig. 2. FNTs showed diameter between 0.3 and 2 μm in agreement with previous reports for FNT nanostructures (Fig. 2). The mean size distribution of FNTs after 24 h of self-assembly in solution measured by Nanosizer were 296 nm. During the process of self-assembly several nanostructures were observed including short nanotubes, nanorods, tangled nanotubes and dendrite assemblies.

Korolkov et al. discussed that each structural type represents sequential steps in the assembled of the large dendritic structures [32]. The FF used in our study formed dendritic nanostructures, therefore we concluded that probably when nanorods come along to form nanotubes during the growth of FNTs, a lateral growth is conducted from this point [6]. This process is more likely to occur on hydrophobic surfaces since the aromatic ring of FF are better spread on these surfaces [11, 14]. AFM images of bare FNTs indicated a smooth outer surface without defects whereas the surface of FNTs modified with FA/MNPs displayed inhomogeneous outer area indicating FA/MNPs clusters on FNTs (Fig. 2). As shown in this image FA/MNPs are embedded in the wall of FNTs suggesting the conjugation of FA/MNPs on FNTs. The optical microscopy image of modified FNTs showed the attachment of FA/MNPs on the outer surface of FNTs (Fig. 3).

FTIR spectra of FNTs conjugated to FA/MNPs showed peaks at wavenumbers of 725 cm^{-1} , which were associated with benzene vibration of FF structure (Fig. 4). The peaks of $1400\text{--}1600\text{ cm}^{-1}$ corresponds to C=C vibration of FA aromatic rings. Peaks observed in the range of $2800\text{--}2980\text{ cm}^{-1}$ are related to C-H of FA aromatic rings. The peak at 693 cm^{-1} is associated with Fe-O bands of MNPs. The absorption bands of FeO has been transmitted from 650 to 693 cm^{-1} indicating the possible interactions of negative charged groups of FeO atoms with positive charged amine groups of FA. FTIR spectrum of these conjugated nanotubes showed an additional peak at 1640 cm^{-1} corresponding to amide II vibration which is due to reaction of carboxylic groups of FA with amine groups of FF.

Interestingly, by diluting FNTs modified with FA/MNPs with deionized water, vesicle FF nanostructures were formed (Fig. 5). The transition from FNTs to vesicles is reversible and dependent on FF concentration. This is attributable to the sufficient free energy association gained by intermolecular interaction at high concentrations of FF (100 mg/ml), while decreased concentrations disassemble the organized arrangement [15]. Formation of vesicle nanostructures is important in cancer treatment since it could enhance the cellular uptake of cargos compared to nanotubes. Conjugated FNTs were further loaded with anti-cancer agent fluorouracil (5-FU) and anti-inflammatory agent flufenamic acid (FFA). FFA was used to study the effect of molecular structure of drugs on morphology of FF. The structure of FFA has similarities to 5-FU and contains fluoro groups with two aromatic rings and therefore it is more hydrophobic compared to 5-FU. Confocal laser scanning microscopy was used to characterize bare FNTs, FNTs conjugated to FA/MNPs, FNTs loaded with 5-FU and FFA (Fig. 6). Bare FNTs displayed weak blue fluorescence emission at $\lambda = 402$ due to their aromatic rings. Bare FNTs showed no fluorescence at $\lambda = 480$ nm.

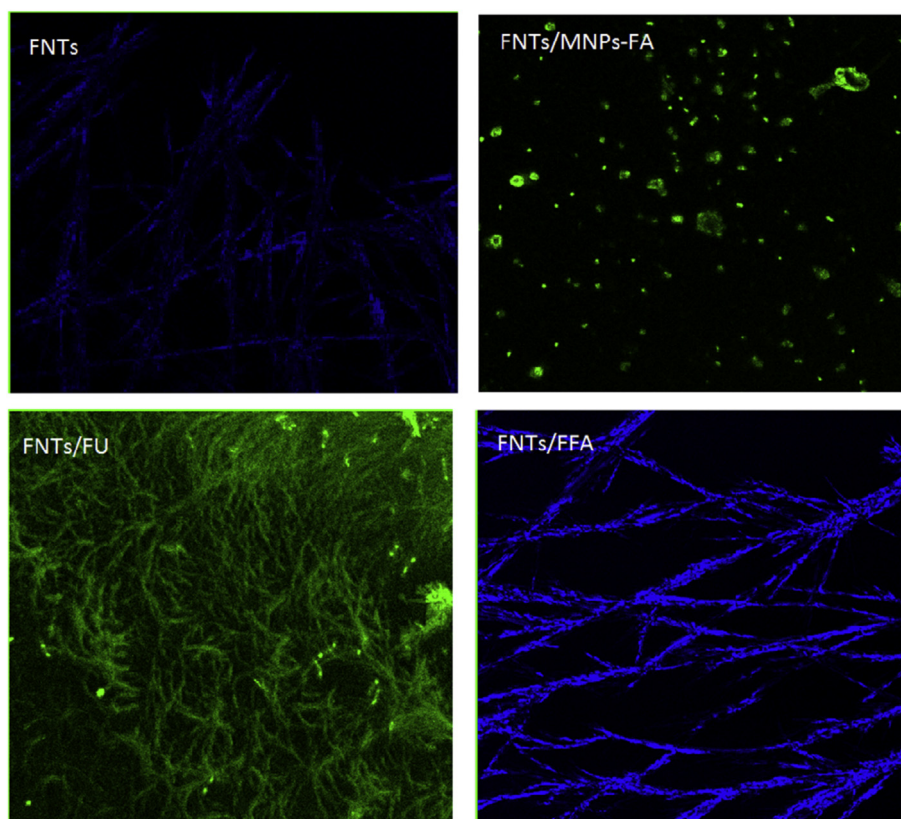


Fig. 6. Confocal laser scanning microscopy of bare FNTs (λ emission = 402); FNTs conjugated to MNPs/FA (λ emission = 480 nm); FNTs loaded with 5-FU and FFA. (λ emission collected at 480, 402 nm).

Covalent FNTs decorated with FA/MNPs exhibited nanoparticles with green fluorescence emission at $\lambda = 480$ nm which indicates distribution of FA on FNT surface. Previous studies have reported similar effects using other molecules, e. g., rhodamine B, folic acid, and hypericin. Castillo et al. used bare FA to conjugate FNTs and observed homogenous distribution of FA on entire FNTs [11]. In our study since FA was decorated with MNPs, distribution of fluorescence on FNTs was found to be on nanoparticles. FNTs loaded with 5-FU displayed green fluorescence emission at $\lambda = 480$ nm corresponding to 5-FU (5-FU is a biomolecule with emission fluorescence at $\lambda = 480$ nm). The emission intensity was localized on FNTs indicating homogenous distribution of 5-FU on FNTs.

FNTs loaded with FFA displayed strong blue fluorescence emission at $\lambda = 402$ corresponding to FFA. The fluorescence intensity was higher compared to bare FNTs indicating FFA has been located on FNTs and has increased the blue fluorescence emission. The morphology of FNTs/5-FU showed dendritic tree-like branched nanostructures (Fig. 6). In contrast, FNTs loaded with FFA displayed large discrete micrometer tubes with high distribution of FFA intensity on these tubes. The observed blue and green fluorescence from FNT conjugates is an evidence that FNTs could host both polar and non-polar cargos, however the hydrophobicity of the cargos

has greatly affected the morphology of FNTs.

Shell of FNTs are strongly hydrophobic because they are composed of aromatic rings from the FF side-chains and the inner core and outer surface have polar sites available to host hydrophilic molecules [15]. Silva et al. reported utilizing FNTs as a platform for drug delivery. Based on characteristic of the drug, colocalization was performed by labeling the nanotubes with both ZnPc (a highly hydrophobic) and rhodamine (a hydrophilic drug) [14]. Their results suggest that the polar RhB was conjugated not only to the external surfaces of the arrays but also at some point to the inside of the structures indicating that FNTs could host both hydrophilic and hydrophobic drugs.

FTIR analysis were carried out on FNTs/5-FU to confirm 5-FU loading and their intermolecular interaction after FA/MNPs conjugation. Typical FTIR spectra of FNTs/5-FU and FA/MNPs are presented in Fig. 7. As shown in Fig. 7a FTIR spectrum of FNTs/5-FU showed characteristic peaks of amine band at 3500 cm^{-1} , which are in good agreement with an antiparallel β -sheet structure [33]. The peak at 725 cm^{-1} represent monosubstituted benzene vibrations from FF structure. After loading FNTs with 5-FU, additional peaks were observed correlated to 5-FU structure. The peaks at $1000\text{--}1400\text{ cm}^{-1}$ are assigned to fluoro groups of 5-FU structure.

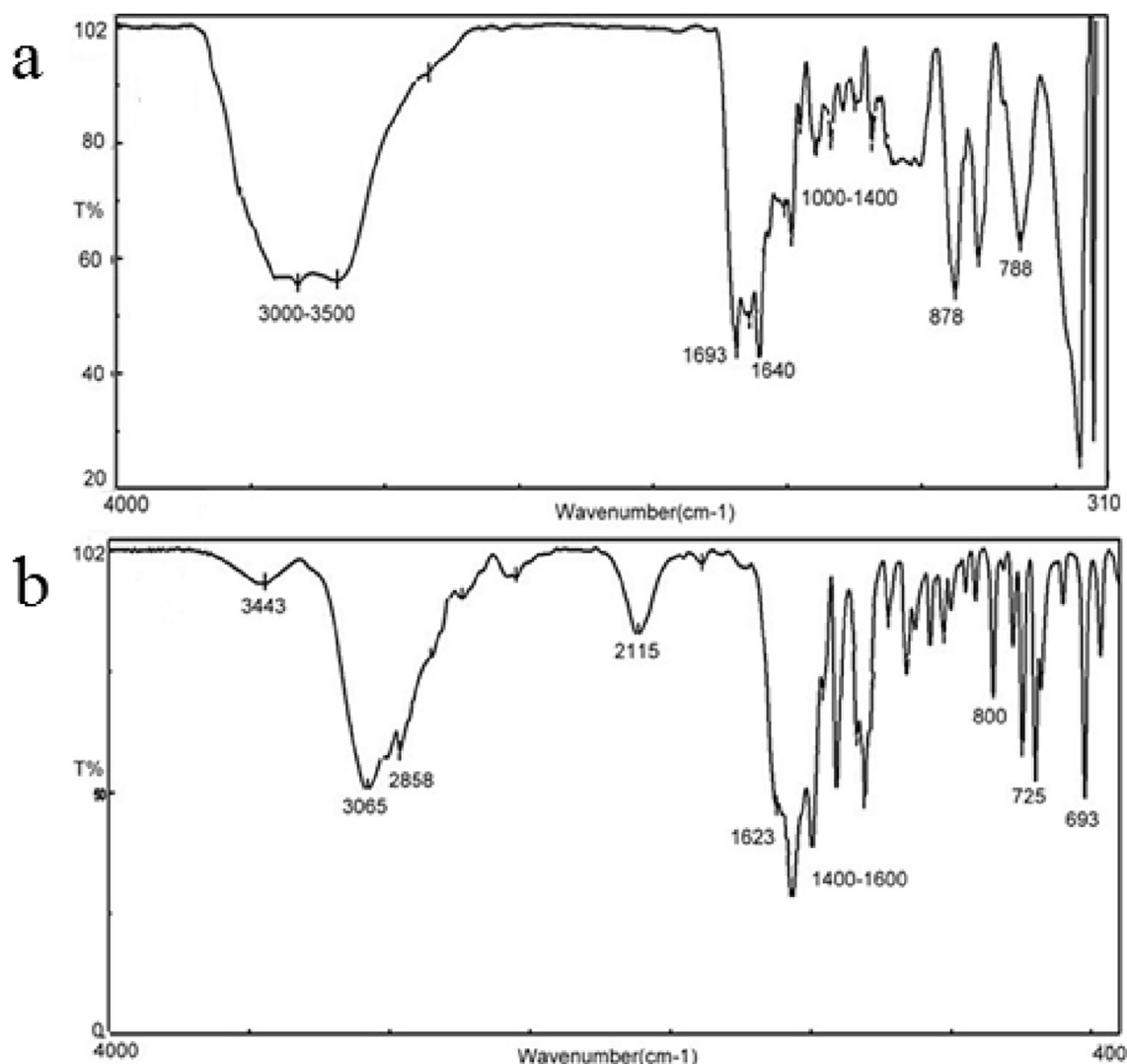


Fig. 7. FTIR spectra of a) FNTs loaded with 5-FU, b) FNTs/MNPs/FA loaded with 5-FU.

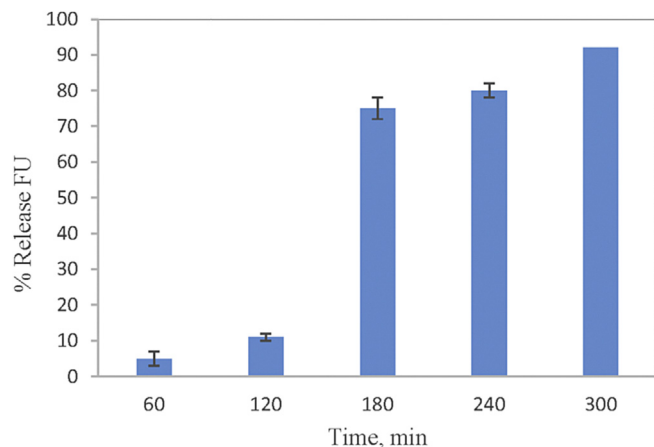


Fig. 8. Release of fluorouracil (5-FU) from FNT hydrogels (75% toluene; 25% ethanol).

Absorption bands around 878 cm^{-1} corresponds to $\text{CF}=\text{CH}$ vibration of 5-FU. The FTIR spectrum of FNTs/5-FU conjugated with FA/MNPs showed peaks at wavelengths of 747, 878, 623, 1000–1400, corresponding to benzene vibration of FF, $\text{CF}=\text{CH}$ of 5-FU, Fe-O, fluoro of 5-FU respectively (Fig. 7). The additional peak at 1623 cm^{-1} in the FNT-FA sample is assigned to vibration of the amide II band that includes C–N stretching of the new amide bond formed between amine group of FNTs and carboxylic group from FA. Moreover, the broad peak at 2500 and 3500 cm^{-1} corresponding to N–H of amines and O–H of carboxylic was removed in this sample indicating their successful interactions. FTIR results confirmed synthesis of FNTs/5-FU conjugated with FA/MNPs.

Release assay of 5-FU from FNTs hydrogels is shown in Fig. 8. Fig. 8 reveals that 5-FU has been released from FNTs within 4 h, and incorporation of 5-FU in FNTs hydrogels has significantly slowed the release rate within the first 2 h. Similar effects have been previously reported by Silva by using rhodamine incorporated in micro nanotubes (MNTs). Silva et al. indicated that 100% of bare rhodamine in absence of MNTs was released in medium within 60 min

whereas only 35% of RhB was released after 60 min in the presence of the FMTs. In a similar approach, Silva reported the release of 90% of RhB from FMTs in 300 min [14]. Our study indicates the potential of L-diphenylalanine nanotubes conjugated to FA/MNPs, as molecular carriers for delivery and release of 5-FU, whereas FA/MNPs provides tremendous application in theranostic agents.

Fig. 9 represents MCF-7 cell mitochondrial activity exposed to FA/MNPs, FA/MNPs/FNTs, and FNTs/5-FU. As shown, the average percentage MTT metabolism of MCF-7 cells after exposure to FA/MNPs and FA/MNPs conjugated to FNTs were reduced from 75% to 63%. The decrease of viability is explained by self-assembly of FNTs in the pericellular space of cancer cells inhibiting cell growth. After loading 5-FU the viability of cells was reduced to 60% due to action of 5-FU as an anti-cancer therapeutic drug.

4. Conclusion

The aim of this work was to synthesis a multicomponent drug carrier based on self-assembled peptide nanotubes (FNTs) modified with folic acid (FA) and magnetic nanoparticles (MNPs) for loading anti-cancer agent fluorouracil (5-FU). FA was added to MNPs during their synthesis and FA/MNPs were attached to FNTs with covalent conjugation through EDC carbodiimide. The ability of functionalized FNTs for hosting anti-cancer drug were evaluated with 5-FU. The complex of FNTs were characterized with AFM, CLSM and FTIR. Self-assembly of FF led to formation of clear nano and microtubular structures with diameter between 0.3 and $2\text{ }\mu\text{m}$. CLSM confirmed emission intensity of FA on MNPs suggesting FA coating on these particles. AFM images indicated the presence of FA/MNPs inside and on the surface wall of FNTs. CLSM image of FNTs loaded with 5-FU exhibited fluorescence signals observed at $\lambda = 480\text{ nm}$, which are characteristic to 5-FU. The morphology of FNTs loaded with 5-FU were tree like dendrite branches, compared to a highly hydrophobic drug flufenamic acid, where long discrete tubes were observed. The new synthesized multicomponent has tremendous potential for application in biomedical field for both targeting and imaging cancer cell and delivering anti-cancer agents for cancer treatment.

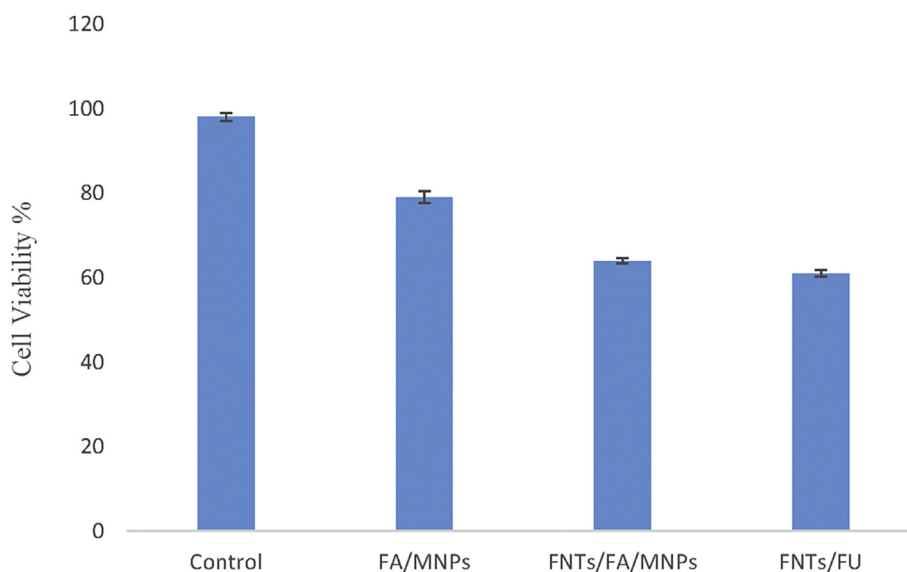


Fig. 9. Cell viability percentage, evaluated by MTT reduction test, after treatment of the (MCF-7) cell line with FA/MNPs, FNTs conjugated to FA/MNPs, and FNTs loaded with 5-FU.

References

- [1] L.J. Yi-Fen Li, S. Pavoola, H. Kavawaa, The nano revolution: bottom-up manufacturing with biomolecules, in smart sensors, actuators, and MEMS, Spain, vol. 6589 (2007).
- [2] G. Whitesides, J. Kriebel, B. Mayers, Self-assembly and nanostructures, nanostructure science and technology, in: WTS (Ed.), *Nanoscale Assembly: Chemical Techniques*, Springer, 2005, pp. 217–238.
- [3] X. Yan, P. Zhu, J. Li, Self-assembly and application of diphenylalanine-based nanostructures, *Chem. Soc. Rev.* 39 (6) (2010) 1877–1890.
- [4] T. Han, J.K. Oh, G. Lee, S. Pyun, S. Kim, Hierarchical assembly of diphenylalanine into dendritic nanoarchitectures, *Colloid Surf. B* 79 (2) (2010) 440–445.
- [5] S. Zhang, Fabrication of novel biomimetic through molecular self-assembly, *Nat. Biotech.* 21 (2003) 10–16.
- [6] T. Zohrabi, N. Habibi, Dendritic peptide nanostructures formed from self-assembly of di-l-phenylalanine extracted from Alzheimer's β -amyloid poly peptides: insights into their assembly process, *Inter J. Pept. Res. Ther.* 21 (4) (2015) 423–431.
- [7] E. Gazit, Self-assembled peptide nanostructures: the design of molecular building blocks and their technological utilization, *Chem. Soc. Rev.* 36 (2007) 1263–1269.
- [8] N. Habibi, F. Caneva Soumetz, M. Giulianelli, L. Pastorino, O. Herrera, S. Francesca, R. Raiteri, C. Ruggiero, Self-assembly and recrystallization of bacterial S-layer proteins of *Bacillus sphaericus* and *Bacillus thuringiensis* on silicone, mica and quartz crystal supports, *Proc. EMBC* (2010) 3739–3742.
- [9] L. Pastorino, N. Habibi, F. Soumetz, M. Giulianelli, C. Ruggiero, Polyelectrolyte multilayers for cell and tissue engineering, *Eur. Cells Mater.* 22 (3) (2011) 66.
- [10] D. Mandal, A.N. Shirazi, K. Parang, Self-assembly of peptides to nanostructures, *Org. Biomol. Chem.* 12 (2014) 3544–3561.
- [11] J.J. Castillo, T. Rindzevicius, K. Wu, M.S. Schmidt, K. Janik, A. Boisen, W. Svendsen, N. Rozlosnik, J. Castillo-Leon, Synthesis and characterization of covalent diphenylalanine nanotube-folic acid conjugates, *J. Nanopart. Res.* 16 (2014) 2525.
- [12] S.K. Smart, A.I. Cassady, G.Q. Lu, A.D.J. Martin, *Biocompat. carbon Nanotub. Carbon* 44 (2006) 1034–1047.
- [13] M. Reches, E. Gazit, Designed aromatic homo-dipeptides: formation of ordered nanostructures and potential nanotechnological applications, *Phys. Biol.* 3 (1) (2006) S10.
- [14] R.F. Silva, D.R. Araujo, E.R. Silva, R.A. Ando, W.A. Alves, L-diphenylalanine microtubes as a potential drug-delivery system: characterization, release kinetics, and cytotoxicity, *Langmuir* 29 (32) (2013) 10205–10212.
- [15] N. Habibi, M.A. Kamaly, H. Shafiee, Self-assembled peptide-based nanostructures: smart nanomaterials toward targeted drug delivery, *Nano Today* 11 (1) (2016) 41–60.
- [16] J. Xie, S. Lee, X. Chen, Nanoparticle-based theranostic agents, *Adv. Drug Deliv. Rev.* 62 (11) (2010) 1064–1079.
- [17] N. Kamaly, T. Kalber, M. Thanou, J.D. Bell, A.D. Miller, Folate receptor targeted bimodal liposomes for tumor magnetic resonance imaging, *Bioconjugate Chem.* 20 (2009) 648–655.
- [18] W. Liu, L. Nie, F. Li, Z.P. Aguilar, H. Xu, Y. Xiong, F. Fen, H. Xu, Folic acid conjugated magnetic iron oxide nanoparticles for nondestructive separation and detection of ovarian cancer cells from whole blood, *Biomater. Sci.* 4 (2016) 159–166.
- [19] I.B. Kim, H. Shin, A.J. Garcia, U.H.F. Bunz, Use of a folate-PPE conjugate to image cancer cells in vitro, *Bioconjugate Chem.* 18 (2007) 815–820.
- [20] E.I. Segal, P. Low, Tumor detection using folate receptor-targeted imaging agents, *Cancer Metastasis Rev.* 27 (2008) 655–6634.
- [21] C. Sun, J.S. Lee, M. Zhang, Magnetic nanoparticles in MR imaging and drug delivery, *Adv. Drug Deliv. Rev.* 60 (11) (2008) 1252–1265.
- [22] Q.L. Jiang, S.W. Zheng, R.Y. Hong, S.M. Deng, L. Guo, R.L. Hu, B. Gao, M. Huang, L.F. Cheng, G.H. Liu, Y.Q. Wa, Folic acid-conjugated Fe_3O_4 magnetic nanoparticles for hyperthermia and MRI in vitro and in vivo, *Appl. Surf. Sci.* 307 (2014) 224–233.
- [23] D. Honarmand, S.M. Ghoreishi, N. Habibi, E. Tayerani Nicknejad, Controlled release of protein from magnetite–chitosan nanoparticles exposed to an alternating magnetic field, *J. Appl. Polym. Sci.* (2015), <http://dx.doi.org/10.1002/app.43335>.
- [24] J.J. Castillo, T. Rindzevicius, L.V. Novoa, W.E. Svendsen, N. Rozlosnik, A. Boisen, P. Escobar, M. Fernando, J. Castillo-Leon, Non-covalent conjugates of single-walled carbon nanotubes and folic acid for interaction with cells over-expressing folate receptors, *J. Mater. Chem. B* 1 (2013) 1475–1481.
- [25] Z.1 Zhang, J. Jia, Y. Lai, Y. Ma, J. Weng, L. Sun, Conjugating folic acid to gold nanoparticles through glutathione for targeting and detecting cancer cells, *Bioorg. Med. Chem.* 18 (15) (2010) 5528–5534.
- [26] L. RJ, L. PS, Delivery of liposomes into cultured KB cells via folate receptor-mediated endocytosis, *J. Biol. Chem.* 269 (5) (1994) 198–204.
- [27] S. Palanikumar, L. Kannammal, B. Meenarathi, Effect of folic acid decorated magnetic fluorescent nanoparticles on the sedimentation of starch molecules, *Inter Nano Lett.* 4 (2014) 104.
- [28] N. Habibi, Functional biocompatible magnetite–cellulose nanocomposite fibrous networks: characterization by Fourier transformed infrared spectroscopy, X-ray powder diffraction and field emission scanning electron microscopy analysis, *Spec. Acta Part A* 136 (2015) 1450–1453.
- [29] N. Habibi, B. Karimi, Fabrication and characterization of zinc oxide nanoparticle coated magnetic iron oxide: effect of S-layers adsorption on surface of oxide, *J. Ind. Eng. Chem.* 20 (5) (2014) 3033–3036.
- [30] N. Habibi, Preparation of biocompatible magnetite–carboxymethyl cellulose nanocomposite: characterization of nanocomposite by FTIR, XRD, FESEM and TEM, *Spectrochim. Acta Part A* 131 (2014) 55–58.
- [31] N. Habibi, Immobilization of bacterial S-layer proteins from *Caulobacter crescentus* on iron oxide-based nanocomposite: synthesis and spectroscopic characterization of zincite-coated Fe_2O_3 nanoparticles, *Spectro Acta A* 125 (2014) 359–362.
- [32] V.V. Korolkov, V.V. Allen, C.J. Roberts, Surface mediated l-phenylalanyl-l-phenylalanine l-phenylalanine, *Farad Discuss.* 166 (2013) 257–267.
- [33] K. Xu, Characterization and Utilization of Self-assembled Diphenylalanine Nanotubes, Dissertation, University of Nottingham, 2011.